Two-photon absorption properties of aggregation systems on the basis of (E)-4-(2-nitrovinyl) benzenamine molecules*

Wang Chuan-Kui(王传奎)[a)†], Zhang Zhen(张 珍)[a)], Ding Ming-Cui(丁明翠)[a)], Li Xiao-Jing(李小静)[a)], Sun Yuan-Hong(孙元红)[b)], and Zhao Ke(赵 珂)[a)]

[a)] *College of Physics and Electronics, Shandong Normal University, Jinan* 250014, *China*

[b)] *Fundamental Division, Shandong Police College, Jinan* 250014, *China*

(Received 6 May 2010; revised manuscript received 18 May 2010)

Aggregation effect caused by the intermolecular hydrogen-bonding interactions on two-photon absorption properties of (E)-4-(2-nitrovinyl) benzenamine molecules is studied at a hybrid density functional level. The geometry optimization studies indicate that there exist two probable conformations for the dimers and three for the trimers. A strong red-shift of the charge-transfer states is shown. The two-photon absorption cross sections of the molecule for certain conformations are greatly enhanced by the aggregation effect, from which a ratio of 1.0:2.6:3.6 is found for the molecule and its dimer and trimer with nearly planar structures. Namely, a 30 or 20 percent increase of the two-photon absorption cross section is observed.

Keywords: two-photon absorption, aggregate effect, hydrogen bonding, organic molecule

PACC: 3380K, 3520G, 3120A

1. Introduction

In recent years, organic molecular materials with large two-photon absorption (TPA) cross sections have attracted increasing attention because of their potential applications in optical power limiting,[1−3] two-photon fluorescence microscopy,[4,5] three-dimensional (3D) optical data storage,[6] nanofabrication,[7] and so on. TPA-based techniques have some specific advantages compared with the conventional one-photon techniques. Thus, organic molecular materials with strong TPA properties, designed using theoretical methods or synthesized in experiment, have become a significant research subject.

Usually experimental studies on TPA materials are performed in solutions, while most of the theoretical investigations focus on a single molecule in gas phase. An accurate description of the condensed phase properties thus needs to consider interactions between the solute and solvent molecules and interactions among the solute molecules. A number of theoretical models, such as Onsager model, local field model, and polarized continuum model, have been developed to simulate the solvent effect.[8−15] Recently, the aggregation effect related to the interactions among the solute molecules has been studied.[16−21] The motivation is that several solute molecules can be aggregated by intermolecular hydrogen bonding, especially for asymmetrical push-pull molecules with strong electron donors and acceptors. Tu *et al.*[17] studied the 1, 3, 5–triamino-2, 4, 6-trinitrobenzene (TATB) molecules using molecular dynamics simulations, and indicated that TATB molecules dissolved in chloroform are aggregated because of the strong hydrogen bonding between the molecules. The aggregation effect on the TPA properties of the molecules was further analysed by Liu *et al.* and a significant influence of the hydrogen bonds on the TPA properties was found.[18,19]

In order to further investigate the significant aggregation effect on the TPA activity of molecules, we take an asymmetrical D-π-A molecule (E)-4-(2-nitrovinyl) benzenamine (BDA)[22] as our basic system, and theoretically design several aggregates, i.e., two dimers and four trimers. The TPA cross sections

*Project supported by the National Basic Research Program of China (Grant No. 2006CB806000), the Open Fund of the State Key Laboratory of High Field Laser Physics (Shanghai Institute of Optics and Fine Mechanics), and the National Natural Science Foundation of China (Grant No. 10974121).

†Corresponding author. E-mail: ckwang@sdnu.edu.cn

© 2010 Chinese Physical Society and IOP Publishing Ltd

of these aggregates are calculated using the density functional response theory.

2. Computational details

The transition probability of the one-photon absorption (OPA) is given by oscillator strength as follows:

$$\delta_{\rm op} = \frac{2\omega_f}{3} \sum_{\alpha} |\langle 0| \mu_\alpha |f\rangle|^2, \tag{1}$$

where μ_α is the electric dipole moment operator, ω_f denotes the excitation energy of the excited state $|f\rangle$, $|0\rangle$ represents the ground state, and the summation is performed over the molecular x, y and z axes.

The TPA transition matrix element of two-photon resonant absorption excited by linearly polarized monochromatic beam is expressed as

$$S_{\alpha\beta} = \sum_i \left[\frac{\langle 0| \mu_\alpha |i\rangle \langle i| \mu_\beta |f\rangle}{\omega_i - \omega_f/2} + \frac{\langle 0| \mu_\beta |i\rangle \langle i| \mu_\alpha |f\rangle}{\omega_i - \omega_f/2} \right], \tag{2}$$

where $\mu_{\alpha(\beta)}$ is the electric dipole moment operator, $|0\rangle$ and $|f\rangle$ are, respectively, the ground and final states, $|i\rangle$ denotes all the intermediate states including the ground state $|0\rangle$, and $\hbar\omega_f$ and $\hbar\omega_i$ are the excitation energies of the states $|f\rangle$ and $|i\rangle$ respectively. The TPA cross section is then given by[23]

$$\delta_{\rm tp} = \sum_{\alpha\beta} [F \times S_{\alpha\alpha} S^*_{\beta\beta} + G \times S_{\alpha\beta} S^*_{\alpha\beta} + H \times S_{\alpha\beta} S^*_{\beta\alpha}], \tag{3}$$

where coefficients F, G and H are related to the incident radiation. For linearly polarized light, F, G and H are 2, 2 and 2, and for circular polarization, they are -2, 3, and 3, respectively. The summation goes over the molecular axes α, $\beta = \{x, y, z\}$.

The TPA cross section directly comparable to experimental measurements is defined as

$$\sigma_{\rm tp} = \frac{4\pi^2 a_0^5 \alpha}{15 c_0} \times \frac{\omega^2 g(\omega)}{\Gamma_f} \delta_{\rm tp}, \tag{4}$$

where a_0 is the Bohr radius, c_0 is the speed of light, α is the fine structure constant, $h\omega$ is the photon energy of the incident light, $g(\omega)$ denotes the spectral line profile, which is assumed to be a δ function here, and Γ_f is the lifetime broadening of the final state, which is generally taken to be 0.1 eV corresponding to a lifetime of few femtoseconds.[24]

The geometry optimizations of all complexes are completed utilizing GAUSSIAN03 program package,[25] and the DALTON quantum chemistry program[26] is used to compute the TPA cross sections. All calculations are carried out at a hybrid density functional theory (B3LYP) level with the 6-31G* basis set.

3. Results and discussion

3.1. Molecular structures

The optimized calculation shows that only two conformations exist for the dimers. The energy difference between the two conformations is about 0.05 eV. There exist four conformations for the trimers, and the energy differences among them are in a range of 0.04 eV. The optimized structures of the BDA molecule (denoted as monomer: M) and the theoretically designed BDA dimers (D1, D2) and BDA trimers (T1–T4) are shown in Fig. 1. As a typical asymmetrical molecule with strong electron donor amino (NH_2) and acceptor nitro (NO_2), the optimized results show that the monomer M has a planar structure with a large permanent dipole moment of $8.89D$. Two hydrogen–oxygen bonds and one hydrogen–nitrogen bond are formed for the dimer D1, in which a good planarity with a relatively large permanent dipole moment of $21.41D$ is displayed. However, there is only one hydrogen–oxygen bond for the dimer D2, where one monomer bends to the opposite dipolar orientation of the other monomer. As a result, its permanent dipole moment is reduced to $6.29D$, which is smaller than that of one monomer.

It is found that the trimers, T1 and T2, have triangular types of configurations. The three molecules in T1 are approximately coplanar, while one of the molecules in T2 deviates from the plane of the other two molecules by a dihedral angle of about 45°. The permanent dipole moments of T1 and T2 are $27.47D$ and $22.63D$, respectively. T3 and T4 have a chain-type feature each; moreover, the structure of T3 is bended while the structure of T4 is extended planar. T4 has a largest permanent dipole moment of $35.8D$, while T3 has a smallest value of $19.13D$. One can anticipate that T4 would have a good TPA performance.

The calculated binding energies for conformations D1, D2, T1, T2, T3, and T4 are 0.406, 0.305, 0.680, 0.721, 0.757, and 0.882 eV, respectively. It can be seen that the conformation D1 is more stable than D2 for the dimmers, and T4 is the most stable among the trimeric ones. As a whole, the trimers are more stable than the dimmers. The large binding energies are mainly caused by the hydrogen bond and dipole–dipole interaction between the monomers.

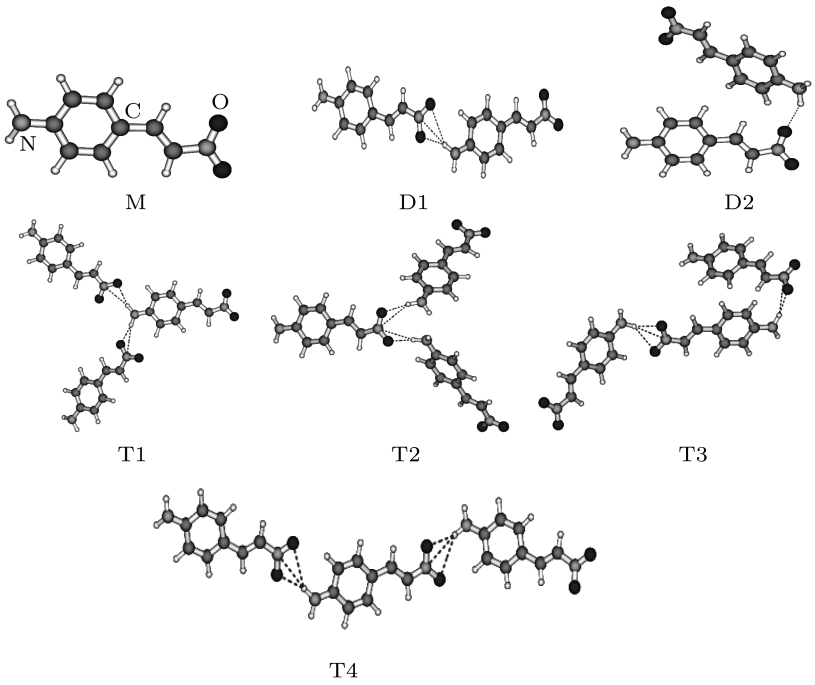


Fig. 1. Optimized structures of the BDA molecule (M), the BDA dimmers (D1, D2), and the BDA trimers (T1–T4).

3.2. One-photon absorption

The calculated linear absorption properties of the BDA molecule and its aggregates for the ten lowest excited states are listed in Table 1. It is observed that only one charge-transfer (CT) state is obvious for the monomer M and the dimmers D1 and D2 in the lower energy regime. However, two CT states for the trimers T1 and T2, three CT states for T3 and four CT states for T4, are obviously recognized. The maximum intensities of OPA for the compounds are 0.6 for M, 1.4 for D1, 1.0 for D2, 1.4 for T1, 1.0 for T2, 1.1 for T3, and 2.0 for T4, and located at 344 nm, 372 nm, 352 nm, 378 nm, 383 nm, 365 nm, and 390 nm, respectively. A red-shift and large one-photon absorption ability for the aggregates compared with those for the monomer are clearly shown.

Table 1. Values of oscillator strength $\delta_{\rm op}$ (a.u.) and corresponding wavelength $\lambda_{\rm op}$ (nm) of the ten lowest excited states for the BDA molecule and its aggregates.

M		D1		D2		T1		T2		T3		T4	
$\lambda_{\rm op}$	$\delta_{\rm op}$	$\lambda_{\rm op}$	$\delta_{\rm op}$	$\lambda_{\rm op}$	$\delta_{\rm op}$	$\lambda_{\rm op}$	$\delta_{\rm op}$	$\lambda_{\rm op}$	$\delta_{\rm op}$	$\lambda_{\rm op}$	$\delta_{\rm op}$	$\lambda_{\rm op}$	$\delta_{\rm op}$
346	0.0	702	0.0	496	0.0	891	0.0	846	0.0	657	0.0	764	0.0
344	0.6	372	1.4	370	0.1	875	0.0	602	0.0	626	0.0	624	0.0
300	0.0	366	0.0	352	1.0	395	0.0	444	0.0	479	0.0	594	0.0
281	0.0	355	0.1	349	0.0	394	0.0	395	0.0	389	0.0	390	2.0
251	0.1	345	0.0	345	0.0	389	0.0	383	1.0	387	0.7	381	0.0
237	0.1	342	0.0	342	0.0	379	0.0	375	0.0	365	1.1	369	0.0
230	0.1	337	0.0	304	0.0	378	1.4	364	0.8	356	0.3	366	0.0
224	0.0	320	0.00	299	0.0	364	0.6	355	0.0	356	0.0	360	0.4
208	0.0	314	0.0	292	0.0	363	0.0	346	0.0	346	0.0	344	0.5
196	0.0	303	0.0	292	0.0	362	0.1	345	0.0	344	0.0	341	0.9

It is interesting to note that the conformation D1 has a large maximum oscillator strength compared with the other conformation D2, and the conformation T4 has the largest maximum oscillator strength among the trimers, which demonstrates that the geometrical structure plays an important role.

3.3. Two-photon absorption

Table 2 lists the calculated TPA cross sections and two-photon wavelengths of the ten lowest excited states, and figure 2 shows the TPA spectra of all complexes with Lorentz broadening. The results indicate that the monomer M has two active TPA states located at 687 nm and 473 nm with the TPA cross sections of 60.4 GM (1 GM=10^{-50} cm^4·s·photon^{-1}) and 53.9 GM, respectively. It is worth while mentioning that the intermolecular charge transfer through the hydrogen-bonding interaction greatly decreases the excitation energies of the aggregates, therefore, the TPA behaviours of dimers and trimers are found at lower energies. Considering the practical applications of TPA techniques, we pay attention to the TPA behaviour with the two-photon wavelength ranging from 600 nm to 1100 nm.

Table 2. Values of TPA cross section $\sigma_{\rm tpa}$ (10^{-50} cm^4·s·photon^{-1}) and two-photon wavelength $\lambda_{\rm tpa}$ (nm) of the ten lowest excited states for the BDA molecule and its aggregates.

M		D1		D2		T1		T2		T3		T4	
$\lambda_{\rm tpa}$	$\sigma_{\rm tpa}$	$\lambda_{\rm tpa}$	$\sigma_{\rm tpa}$	$\lambda_{\rm tpa}$	$\sigma_{\rm tpa}$	$\lambda_{\rm tpa}$	$\sigma_{\rm tpa}$	$\lambda_{\rm tpa}$	$\sigma_{\rm tpa}$	$\lambda_{\rm tpa}$	$\sigma_{\rm tpa}$	$\lambda_{\rm tpa}$	$\sigma_{\rm tpa}$
693	0.1	1397	9.2	989	4.2	1779	19.0	1682	38.6	1309	8.2	1527	0.1
687	60.4	741	159.4	738	61.5	1742	11.4	1201	15.3	1249	0.0	1243	16.5
602	0.0	730	15.0	703	15.5	788	0.4	886	10.0	955	0.6	1183	10.1
560	0.3	709	19.9	697	0.6	788	0.1	788	0.7	775	0.3	778	215.7
501	7.1	689	0.0	691	0.2	775	0.0	763	68.3	770	106.5	761	6.1
473	53.9	685	0.0	685	0.1	756	0.4	752	0.1	727	43.2	740	0.0
459	17.0	674	4.4	608	0.2	754	115.1	725	49.7	711	32.6	729	9.8
446	0.7	639	27.4	597	0.0	725	0.0	707	0.2	709	3.5	719	53.8
416	0.0	628	14.7	583	0.2	725	41.2	693	0.1	691	0.1	681	7.3
391	0.0	606	4.2	582	0.0	723	0.1	689	0.0	676	0.0	674	0.1

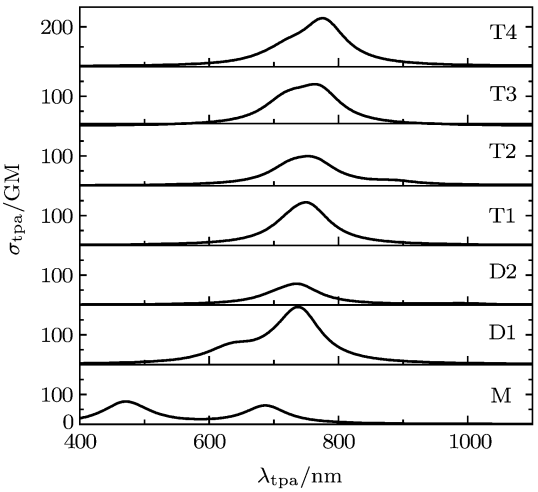


Fig. 2. Calculated TPA spectra of the BDA molecule and its aggregates.

It can be seen from the TPA spectra shown in Fig. 2 that there is only one intensive broad TPA peak for each aggregate in the wavelength region of interest. The maximum TPA cross section, 159.4 GM, of D1 at 742 nm is about 2.6 times that of the monomer M. Compared with D1, D2 has a small TPA cross section maximum, 61.5 GM, located at 738 nm. The reason for such a small value is that the structure of D2 is distorted, which blocks the charge transfer through the hydrogen-bonding network. The results demonstrate that the TPA properties are sensitive to the conformations of the dimers.

For the trimers, T4 has the largest TPA cross section maximum of 215.7 GM at 778 nm, nearly 3.6 times that of the monomer M, while T2 displays the smallest TPA cross section maximum of 68.3 GM at 763 nm. Furthermore, the dominating TPA states for T1 and T3, with TPA cross sections of 115.1 GM and 106.5 GM, are respectively at 754 nm and 770 nm. It is further proven that a coplanar structure in the system is helpful for enhancing the TPA intensities.

As shown above, the structures of monomer M, dimer D1, and trimer T4 each have a planar feature, and the ratio of the maximal TPA cross sections among them is 1.0:2.6:3.6. It should be noted that the TPA cross sections of the aggregated systems are not the sum of individual molecule cross sections. The TPA cross sections of D1 and T4 are enhanced by the hydrogen-bond interaction, namely, the aggregation effect plays a role in enhancing the TPA intensity.

3.4. Charge transfer process

We analyse the charge distribution of the molecular orbits that are involved in the two-photon excitation for the dominating TPA state of the trimer T4 (Fig. 3). It is noted that three different processes make contributions to the two-photon excitation. The electron transition from HOMO-2 (highest occupied molecular orbital) to LUMO (lowest unoccupied molecular orbital) corresponds to the charge transfer within the left molecule, the transition from HOMO-1 to LUMO+1 is generated from the charge transfer of the central molecule, and the transition from HOMO to LUMO+2 concentrates on the charge transfer inside the right molecule. It is interesting to observe that for each charge-transfer process, the charge is obviously moving from the electron donor amino group to the acceptor nitro group. To sum up, the presence of hydrogen bonds changes the molecular charge distribution, and therefore affects the TPA property of aggregates.

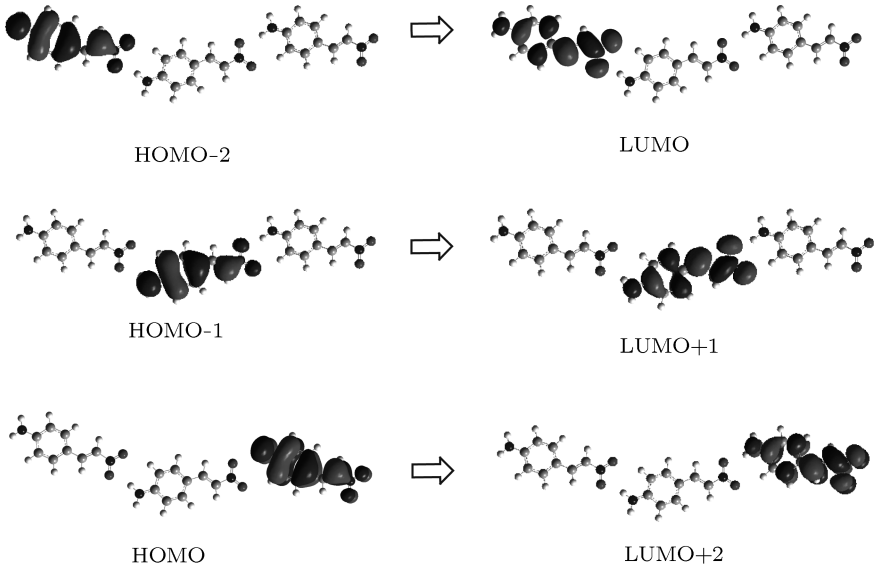


Fig. 3. Molecular orbits involved in the strongest TPA excitations of the trimer T4.

Table 3. Values of wavelength λ_{op} (nm) of the six lowest excited states for the BDA molecule and the bimer D1 and the trimer T4 with other basis set and hybrid exchange-correlation functions.

Mol.	B3LYP 6-31G*	B3LYP 6-31G**	B3PW91 6-31G*	B3P86 6-31G*
	λ_{op}	λ_{op}	λ_{op}	λ_{op}
M	346.0	346.1	341.6	340.8
	344.2	344.7	340.8	340.6
	300.8	300.9	297.5	296.4
	281.2	281.2	278.4	278.1
	251.0	251.5	249.2	249.1
	236.9	236.9	234.5	234.4
D1	702.3	705.9	706.8	702.7
	371.6	372.3	367.9	368.0
	366.1	365.7	358.9	361.7
	355.5	356.0	352.2	351.7
	344.6	344.7	342.8	341.7
	342.0	342.3	339.2	338.5
T4	764.0	770.2	734.3	770.2
	624.1	621.3	606.2	621.3
	594.4	593.4	578.6	593.4
	390.0	386.2	385.0	386.2
	381.4	378.0	370.3	378.0
	369.5	369.7	363.6	369.7

The calculations presented above have been performed with exchange-correlated hybrid function B3LYP and 6-31G* basis set. In order to check the validity of the results, we also choose larger basis sets and other hybrid exchange-correlation functions for calculations (see Table 3). From Table 3, one can see that the excitation wavelengths are changed a little for larger basis set and other hybrid exchange-correlation functions. Taken the CT state of the trimer T4 as an example, when the basis set is enlarged, the excitation wavelength has a shift of 3.8 nm for 6-31G**. When a hybrid function B3PW91 is used, the excitation wavelength has a shift of 5 nm, while for B3P86, the shift is 3.8 nm. The additional calculations thus prove the reliability of the results obtained at B3LYP/6-31G* level.

4. Conclusion

The aggregation effect on the TPA properties of (E)-4-(2-nitrovinyl)benzenamine molecules is studied using the quadratic response theory at a B3LYP level. Concerning the small aggregates, we predict that two conformations of the dimers and four conformations of the trimers exist in view of energy. It is found that the formation of the hydrogen bond has a strong influence on the electronic structure and the TPA properties of the molecule. The TPA spectrum is pushed to the longer wavelength by the hydrogen bond, and the TPA cross section is sensitive to the conformation of the aggregation. For certain conformations, a large enhancement of the TPA cross section of the molecule is observed.

References

[1] Ehrlich J E, Wu X L, Lee I S, Hu Z H, Röckel H, Marder S R and Perry J W 1997 *Opt. Lett.* **22** 1843

[2] Said A A, Wamsely C, Hagan D J, Van Stryland E W, Reinhardt B A, Roderer P and Dillard A G 1994 *Chem. Phys. Lett.* **228** 646

[3] He G S, Gvishi R, Prasad P N and Reinhardt B 1995 *Opt. Commun.* **117** 133

[4] Denk W, Strickler J H and Webb W W 1990 *Science* **248** 73

[5] Rentzepis P M and Parthenopoulos S D A 1989 *Science* **245** 843

[6] Strickler J H and Webb W W 1991 *Opt. Lett.* **16** 1780

[7] Cumpston B H, Anthavel S P, Barlow S, Dyer D L, Ehrlich J E, Erskine L L, Heikal A A, Kuebler S M, Lee I Y S, McCord-Maughon D, Qin J, Rockel H, Rumi M, Wu X L, Marder S R and Perry J W 1999 *Nature* **398** 51

[8] Ferrighi L, Frediani L, Fossgaard E and Ruud K 2007 *J. Chem. Phys.* **127** 244103

[9] Wang C K, Zhao K, Su Y, Ren Y, Zhao X and Luo Y 2003 *J. Chem. Phys.* **119** 1208

[10] Miertus S, Scrocco E and Tomasi J 1981 *Chem. Phys.* **55** 117

[11] Tomasi J and Persico M 1994 *Chem. Rev.* **94** 2027

[12] Cammi R, Cossi M and Tomasi J 1996 *J. Chem. Phys.* **104** 4611

[13] Wang C K, Huang X M, Xing X J and Gao Y 2007 *Chin. Phys.* **16** 3323

[14] Guo Y H, Sun Y H, Tao L M, Zhao K and Wang C K 2005 *Chin. Phys.* **14** 2202

[15] Wang C K, Wang Y H, Su Y and Luo Y 2003 *J. Chem. Phys.* **119** 4409

[16] Datta A and Pati S K 2003 *J. Chem. Phys.* **118** 8420

[17] Tu Y Q, Luo Y and Ågren H 2005 *J. Phys. Chem.* B **109** 16730

[18] Sun Y H, Li J, Zhao K and Wang C K 2010 *Chin. Phys.* B **19** 044207

[19] Liu K, Wang Y H, Tu Y Q, Ågren H and Luo Y 2008 *J. Phys. Chem.* B **112** 4387

[20] Liu Z J, Shao P, Huang Z, Liu B, Chen T and Qin J G 2008 *Chem. Commun.* **19** 2260

[21] Zhao K, Tu Y Q and Luo Y 2009 *J. Phys. Chem.* B **113** 10271

[22] Kanis D R, Ratner M A and Marks T J 1994 *Chem. Rev.* **94** 195

[23] Monson P R and McClain W M 1970 *J. Chem. Phys.* **53** 29

[24] Albota M, Beljonne D, Brédas J L, Ehrlich J E, Fu J Y, Heikal A A, Hess S E, Kogej T, Levin M D, Marder S R, McCord-Maughon D, Perry J W, Röckel H, Rumi M, Subramaniam G, Webb W W, Wu X L and Xu C 1998 *Science* **281** 1653

[25] Frisch M J, Trucks G W, Schlegel H B, *et al.* 2004 *Gaussian* 03, Revision D.02 Wallingford, CT: Gaussian Inc.

[26] Angeli C, Bak K L, Bakken V, *et al.* 2005 *Dalton2.0*, Release2.0